ISES
Institute for Sustainable Energy Systems

HM LMRES

Laboratory for Mechatronic and Renewable Energy Systems

Nonlinear current control with optimal reference voltage saturation for electrically excited synchronous machines

Niklas Monzen, Pascal Seitter, and Christoph M. Hackl †

Hochschule München (HM) University of Applied Sciences

Introduction

In drive control, voltage constraints play a critical role, as the limitations of power electronics and DC link voltage restrict the feasible output range. Modern control methods such as model predictive control (MPC) inherently incorporate these constraints into the control law. However, in industrial applications, traditional field-oriented control (FOC) with proportional-integral (PI) controllers remains the dominant approach. A major drawback of PI-based schemes is their limited capability to handle constraints effectively. Here, voltage constraints are typically addressed using anti-windup strategies with classical reference voltage saturation (CRVS) [1]. However, CRVS often degrades current control performance, particularly in the presence of cross-coupling effects [4]. To overcome these limitations, an optimal reference voltage saturation (ORVS) strategy for nonlinear PI-based current control was proposed in [3] for reluctance synchronous machines (RSMs), demonstrating excellent simulation performance. Extending this approach to electrically excited synchronous machines (EESMs) is more challenging, as the exciter current introduces an additional control variable with its own constraints.

Contributions: This work develops a control framework for an EESM featuring

- a nonlinear PI-based current control system, and
- an integrated ORVS strategy.

Modeling

Machine Model: Nonlinear EESM in the rotor-aligned (d,q)-reference frame [2].

$$\left.\begin{aligned} \tfrac{\mathrm{d}}{\mathrm{d}t}\boldsymbol{\psi}_{\mathrm{s,e}}^{dqe} &= \boldsymbol{u}_{\mathrm{s,e}}^{dqe} - \boldsymbol{R}_{\mathrm{s,e}}^{dqe}\boldsymbol{i}_{\mathrm{s,e}}^{dqe} - \omega_{\mathrm{p}}\boldsymbol{J}_0\boldsymbol{\psi}_{\mathrm{s,e}}^{dqe}, \\ \tfrac{\mathrm{d}}{\mathrm{d}t}\omega_{\mathrm{m}} &= \tfrac{1}{\Theta_{\mathrm{m}}}\big(m_{\mathrm{m}} - m_{\mathrm{l}}\big), \\ \tfrac{\mathrm{d}}{\mathrm{d}t}\phi_{\mathrm{m}} &= \omega_{\mathrm{m}} \end{aligned}\right\}$$

with $\boldsymbol{J}_0 := \left[\begin{smallmatrix} 0 & -1 & 0 \\ 1 & 0 & 0 \\ 0 & 0 & 0 \end{smallmatrix}\right]$, stator and exciter voltages $\boldsymbol{u}_{\mathrm{s,e}}^{dqe} := (u_{\mathrm{s}}^{d}, u_{\mathrm{s}}^{d}, u_{\mathrm{e}}^{e})^\top$, stator and exciter currents $\boldsymbol{i}_{\mathrm{s,e}}^{dqe} := (i_{\mathrm{s}}^{d}, i_{\mathrm{s}}^{q}, i_{\mathrm{e}}^{e})^\top$, stator and exciter flux linkages $\boldsymbol{\psi}_{\mathrm{s,e}}^{dqe} := (\psi_{\mathrm{s}}^{d}, \psi_{\mathrm{s}}^{q}, \psi_{\mathrm{e}}^{e})^\top$, resistance matrix $\boldsymbol{R}_{\mathrm{s,e}}^{dqe} \in \mathbb{R}^{3\times 3}$, differential inductance matrix $\boldsymbol{L}_{\mathrm{s,e}}^{dqe} := \frac{\mathrm{d}}{\mathrm{d}(\boldsymbol{i}_{\mathrm{s,e}}^{dqe})^\top}\boldsymbol{\psi}_{\mathrm{s,e}}^{dqe}$, induced voltage vector $\boldsymbol{\delta}_{\mathrm{s,e}}^{dqe} := \omega_{\mathrm{m}}\frac{\mathrm{d}}{\mathrm{d}\phi_{\mathrm{m}}}\boldsymbol{\psi}_{\mathrm{s,e}}^{dqe}$, mechanical angular velocity $\omega_{\mathrm{m}} := \frac{\omega_{\mathrm{p}}}{n_{\mathrm{p}}}$ (i.e., electrical angular velocity ω_{p} divided by pole pair number n_{p}), inertia constant Θ_{m}, average machine torque $m_{\mathrm{m}} := \frac{2}{3\kappa^2}n_{\mathrm{p}}(\boldsymbol{i}_{\mathrm{s,e}}^{dqe})^\top\boldsymbol{J}_0\boldsymbol{\psi}_{\mathrm{s,e}}^{dqe}$, Clarke transformation factor $\kappa \in \{2/3, \sqrt{2/3}\}$, load torque m_{l} and mechanical angle ϕ_{m}.

Overall control scheme

Overview: Proposed nonlinear current control system.

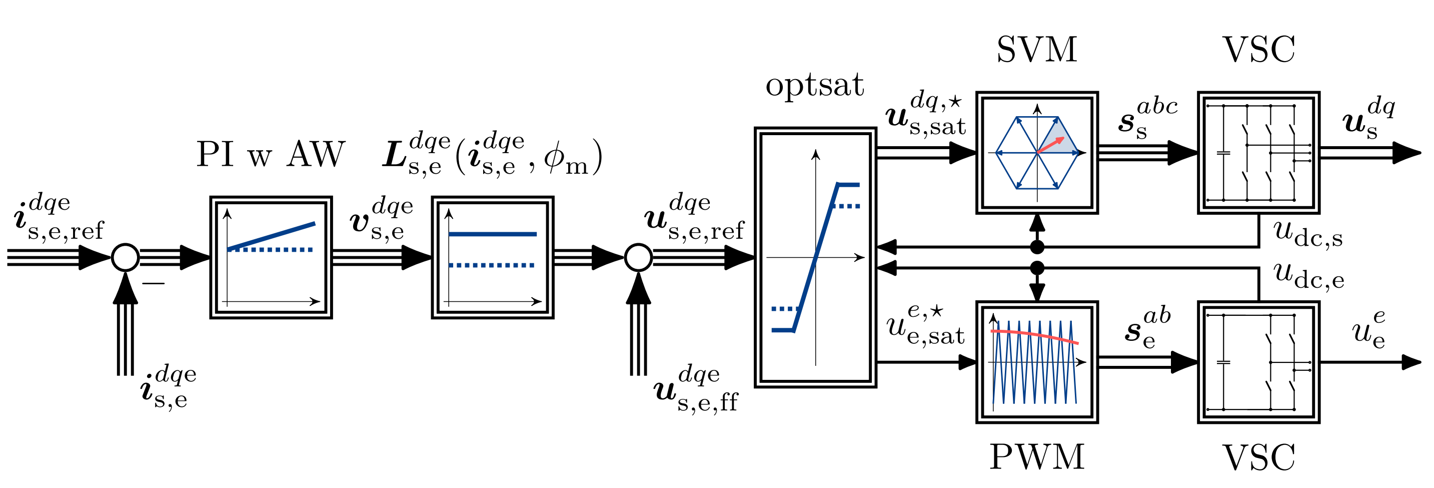

Figure 1. Block diagram of the proposed current control system, integrating optimal reference voltage saturation, input/output linearization, and proportional-integral controllers with anti-windup.

Current control system

Input/Output (I/O) Linearization:

$$\boldsymbol{u}_{\mathrm{s,e,ref}}^{dqe} := \boldsymbol{L}_{\mathrm{s,e}}^{dqe}\boldsymbol{v}_{\mathrm{s,e}}^{dqe} + \boldsymbol{u}_{\mathrm{ff}}^{dqe}, \quad \boldsymbol{u}_{\mathrm{ff}}^{dqe} := \boldsymbol{R}_{\mathrm{s,e}}^{dqe}\boldsymbol{i}_{\mathrm{s,e}}^{dqe} + \omega_{\mathrm{p}}\boldsymbol{J}_0\boldsymbol{\psi}_{\mathrm{s,e}}^{dqe} + \boldsymbol{\delta}_{\mathrm{s,e}}^{dqe}.$$

Assuming $\boldsymbol{u}_{\mathrm{s,e}}^{dqe} \approx \boldsymbol{u}_{\mathrm{s,e,ref}}^{dqe}$, the current dynamics reduce to $\frac{\mathrm{d}}{\mathrm{d}t}\boldsymbol{i}_{\mathrm{s,e}}^{dqe}(\boldsymbol{u}_{\mathrm{s,e}}^{dqe}) = \boldsymbol{v}_{\mathrm{s,e}}^{dqe}$.

Closed-Loop Control: With a conventional PI controller, the closed-loop transfer function becomes

$$F_{\mathrm{CL}}^{z}(s) = \frac{i_y^z(s)}{i_{y,\mathrm{ref}}^z(s)} = \left(1 + \frac{k_{\mathrm{p}}^z}{k_{\mathrm{i}}^z}s\right)\frac{k_{\mathrm{i}}^z}{s^2 + k_{\mathrm{i}}^z s + k_{\mathrm{i}}^z}, \quad (y,z) \in \{(\mathrm{s},d),\,(\mathrm{s},q),\,(\mathrm{e},e)\}.$$

Tuning: The closed-loop dynamics correspond to a second-order system with a differential term. Simple *pole placement* allows direct tuning via the controller gains k_{p}^z and k_{i}^z.

Optimal reference voltage saturation

Feasible Voltage Set: The reference voltage $\boldsymbol{u}_{\mathrm{s,e,ref}}^{dqe}$ is admissible only if contained in

$$\mathbb{F}_{\mathrm{u}} := \left\{(u_1, u_2, u_3)^\top \in \mathbb{R}^3 \;\middle|\; \|(u_1, u_2)\| \leqslant u_{\mathrm{s,max}},\; |u_3| \leqslant u_{\mathrm{e,max}}\right\}.$$

Saturation Principle: If $\boldsymbol{u}_{\mathrm{s,e,ref}}^{dqe} \notin \mathbb{F}_{\mathrm{u}}$, the saturated voltage $\boldsymbol{u}_{\mathrm{s,e,sat}}^{dqe}$ should preserve the direction of the current dynamics:

$$\tfrac{\mathrm{d}}{\mathrm{d}t}\boldsymbol{i}_{\mathrm{s,e}}^{dqe}(\boldsymbol{u}_{\mathrm{s,e,sat}}^{dqe}) = (1-\zeta)\,\tfrac{\mathrm{d}}{\mathrm{d}t}\boldsymbol{i}_{\mathrm{s,e}}^{dqe}(\boldsymbol{u}_{\mathrm{s,e,ref}}^{dqe}), \quad \zeta \in [0,1],$$

which yields

$$\boldsymbol{u}_{\mathrm{s,e,sat}}^{dqe} = (1-\zeta)\,\boldsymbol{L}_{\mathrm{s,e}}^{dqe}\boldsymbol{v}_{\mathrm{s,e}}^{dqe} + \boldsymbol{u}_{\mathrm{ff}}^{dqe}.$$

Optimal Saturation: The optimal scaling factor $\zeta^\star$ minimizes the deviation in current dynamics subject to input constraints, and a closed-form solution can be obtained by solving:

$$\begin{aligned} \zeta^\star = \arg\min_{\zeta}\; & \zeta \\ \text{s.t. }\; & \tfrac{\mathrm{d}}{\mathrm{d}t}\boldsymbol{i}_{\mathrm{s,e}}^{dqe}(\boldsymbol{u}_{\mathrm{s,e,sat}}^{dqe}) - (1-\zeta)\tfrac{\mathrm{d}}{\mathrm{d}t}\boldsymbol{i}_{\mathrm{s,e}}^{dqe}(\boldsymbol{u}_{\mathrm{s,e,ref}}^{dqe}) = \boldsymbol{0}_3, \\ & \|\boldsymbol{u}_{\mathrm{s,sat}}^{dq}\|^2 \leqslant u_{\mathrm{s,max}}^2, \\ & u_{\mathrm{e,sat}}^2 \leqslant u_{\mathrm{e,max}}^2. \end{aligned}$$

Validation

Setup: Simulations were performed on a real nonlinear EESM.

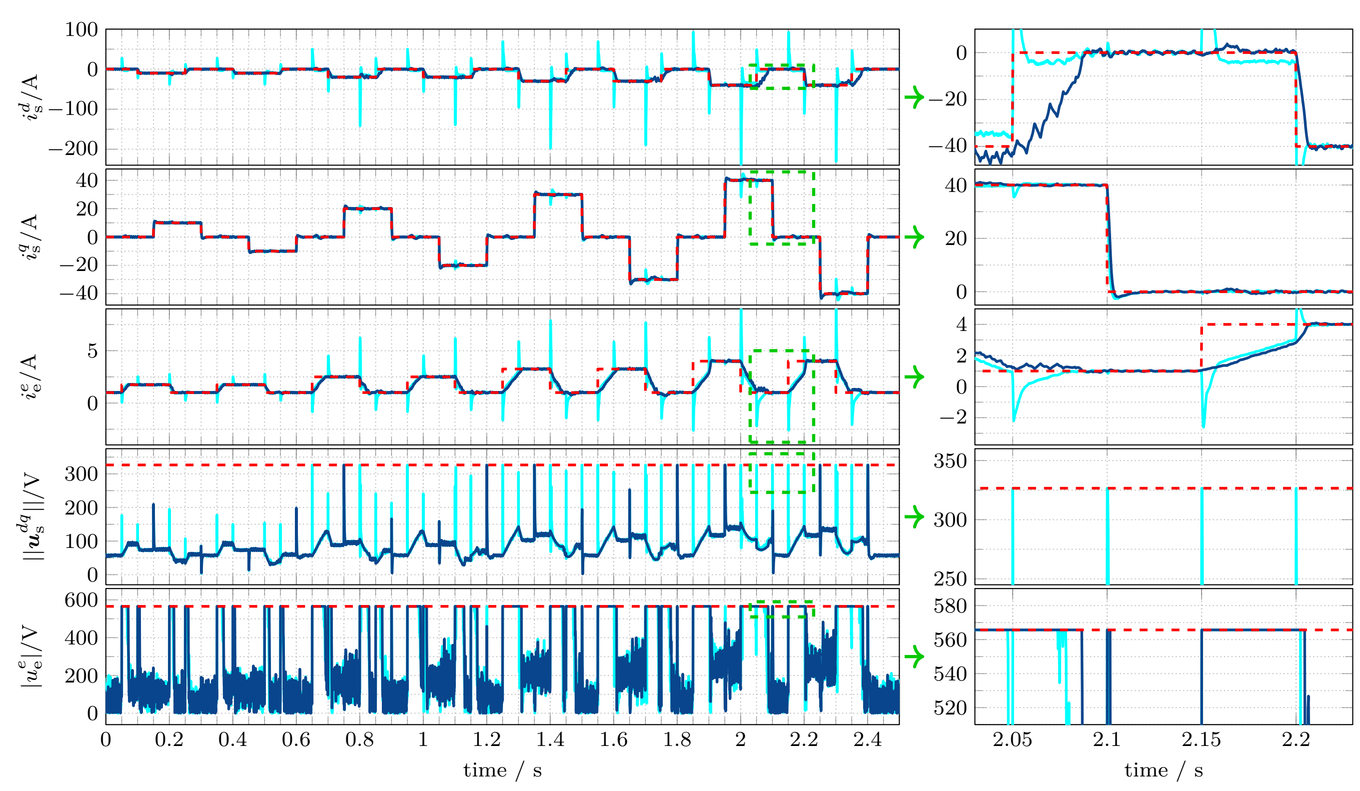

Figure 2. Time series results of the proposed current control system for the EESM, showing stator (d,q)-currents, exciter current, and reference voltage amplitudes, colorized by the applied reference voltage saturation approaches: CRVS [—], ORVS [—]. Their references are shown in [- - -], along with stator voltage constraints $u_{\mathrm{s,max}}$ [- - -], and the exciter voltage constraint $u_{\mathrm{dc,e}}$ [- - -]. Left: Full-time series. Right: Zoomed-in views of the regions highlighted by [- - -].

Conclusion

- Nonlinear current control system using I/O linearization and PI controllers
- ORVS minimizes the gap between desired and feasible current dynamics while:
  - preserving the desired current change direction
  - considering stator and exciter voltage constraints
- High-fidelity simulations show ORVS outperforms classical methods by:
  - improving current tracking accuracy
  - significantly reducing cross-coupling effects

References

[1] Phil March and Matthew C. Turner. Anti-windup compensator designs for nonsalient permanent-magnet synchronous motor speed regulators. 45(5):1598–1609.

[2] Niklas Monzen and Christoph M. Hackl. Artificial neural network based optimal feedforward torque control of electrically excited synchronous machines. In *2023 IEEE 32nd International Symposium on Industrial Electronics (ISIE)*. IEEE, 2023.

[3] Niklas Monzen and Christoph M. Hackl. Optimal reference voltage saturation for nonlinear current control of synchronous machine drives. In *2024 IEEE 21st International Power Electronics and Motion Control Conference (PEMC)*, pages 1–6. IEEE, 2024.

[4] Johannes Reinhard, Klaus Löhe, and Knut Graichen. Optimal dynamic current control for externally excited synchronous machines. In *2024 IEEE Conference on Control Technology and Applications (CCTA)*, pages 146–152. IEEE.

† Corresponding author: Prof. Dr.-Ing. habil. Christoph M. Hackl   +49 (0)89 1265-3417   christoph.hackl@hm.edu   https://lmres.ee.hm.edu